

Analytical theory of wave propagation through stacked fishnet metamaterials

R. Marqués,^{1*} L. Jelinek,¹ F. Mesa,² and F. Medina¹

¹ *Departamento de Electrónica y Electromagnetismo, Universidad de Sevilla
Avd. Reina Mercedes, 41012 Sevilla (Spain)*

² *Departamento de Física Aplicada I, ETSII, Universidad de Sevilla
Avd. Reina Mercedes, 41012 Sevilla (Spain)*

[*marques@us.es](mailto:marques@us.es)

Abstract: This work analyzes the electromagnetic wave propagation through periodically stacked fishnets from zero frequency to the first Wood's anomaly. It is shown that, apart from Fabry-Perot resonances, these structures support two transmission bands that can be backward under the appropriate conditions. The first band starts at Wood's anomaly and is closely related to the well-known phenomena of extraordinary transmission through a single fishnet. The second band is related to the resonances of the fishnet holes. In both cases, the in-plane periodicity of the fishnet cannot be made electrically small, which prevents any attempt of homogenization of the structure along the fishnet planes. However, along the normal direction, even with very small periodicity transmission is still possible. An homogenization procedure can then be applied along this direction, thus making that the structure can behave as a backward-wave transmission line for such transmission bands. Closed-form design formulas will be provided by the analytical formulation here presented. These formulas have been carefully validated by intensive numerical computations.

© 2009 Optical Society of America

OCIS codes: (160.3918) Metamaterials; (050.2065) Effective medium theory; (160.1245) Artificially engineered materials; (160.5298) Photonic crystals

References and links

1. S. Zhang, W. Fan, K. J. Malloy, and S. R. J. Brueck, "Near-infrared double negative metamaterials," *Opt. Express* **13**, 4922-4930 (2005).
2. S. Zhang, W. Fan, N. C. Panoiu, K. J. Malloy, R. M. Osgood, and S. R. J. Brueck, "Experimental Demonstration of Near-Infrared Negative-Index Metamaterials," *Phys. Rev. Lett.* **95**, 137404 (2005).
3. M. Beruete, M. Sorolla, and I. Campillo "Left-handed extraordinary optical transmission through a photonic crystal of subwavelength hole arrays," *Opt. Express* **14**, 5445-5455 (2006).
4. M. Beruete, I. Campillo, M. Navarro-Cía, F. Falcone, and M. Sorolla "Molding left- or right-handed metamaterials by stacked cutoff metallic hole arrays," *IEEE Trans. Microwave Theory Tech.* **55**, 1514-1521 (2007).
5. M. Navarro-Cía, M. Beruete, M. Sorolla, and I. Campillo, "Negative refraction in a prism made of stacked subwavelength hole arrays," *Opt. Express* **16**, 560-566 (2008).
6. G. Dolling, Ch. Enkrich, M. Wegener, C. M. Soukoulis, and S. Linden "Low-loss negative-index metamaterial at telecommunication wavelengths," *Opt. Lett.* **31** 1800-1802 (2005).
7. J. Valentine, S. Zhang, T. Zentgraf, E. Ulin-Avila, D. A. Genov, G. Bartal, and X. Zhang, "Three-dimensional optical metamaterial with a negative refractive index," *Nature (London)* **455**, 299-300 (2008).
8. G. Dolling, M. Wegener, C. M. Soukoulis, and S. Linden, "Negative-index metamaterial at 780 nm wavelength," *Opt. Lett.* **32** 53-55 (2007).
9. T. W. Ebbesen, H. J. Lezec, H. F. Ghaemi, T. Thio, and P. A. Wolff, "Extraordinary optical transmission through sub-wavelength hole arrays," *Nature (London)* **391**, 667-669 (1998).

10. D. R. Smith, W. J. Padilla, D. C. Vier, S. C. Nemat-Nasser, and S. Schultz, "Composite medium with simultaneously negative permeability and permittivity," *Phys. Rev. Lett.* **84**, 4184-4187 (2000).
 11. A. Mary, S. G. Rodrigo, F. J. Garcia-Vidal, and L. Martin-Moreno, "Theory of negative-refractive-index response of double-fishnet structures," *Phys. Rev. Lett.* **101**, 103902 (2008).
 12. F. Medina, F. Mesa, and R. Marqués, "Extraordinary transmission through arrays of electrically small holes from a circuit theory perspective," *IEEE Trans. Microwave Theory Tech.* **56**, 3108-3120 (2008).
 13. R. Marqués, F. Mesa, L. Jelinek, and F. Medina "Analytical theory of extraordinary transmission through metallic diffraction screens perforated by small holes," *Opt. Express* **17**, 5571-5579 (2009)
 14. J. D. Jackson, *Classical Electrodynamics*, (Edt. Wiley, New York 1999), 3rd Ed.
 15. R. Gordon, "Bethe's aperture theory for arrays," *Phys. Rev. A* **76**, 053806 (2007).
 16. R. F. Collin *Field Theory of Guided Waves*, (Edt. IEEE Press, New York 1991), 2nd Ed.,
 17. S. Ramo, J. R. Whinnery, and T. Van Duzer, *Fields and Waves in Communication Electronics*, (Edt. Wiley, New York 1994), 3rd Ed., pp.263-264.
 18. G. V. Eleftheriades, O.Siddiqui, and A. K. Iyer, "Transmission line models for negative refractive index media and associated implementations without excess resonators," *IEEE Microwave and Wirel. Compon. Lett.* **13**, 51-53 (2003).
-

1. Introduction

Stacked metallic plates perforated by periodic hole arrays –the so-called fishnet structures– were first proposed to obtain low-loss negative refractive index metamaterials at near-infrared frequencies [1, 2], and subsequently demonstrated at microwave and terahertz frequencies (where metals are almost perfect conductors) [3–5], in the far-infrared frequency range [6, 7], and in the visible range [8]. This behavior was first observed in double fishnet structures [1, 2, 6, 8], and later in multilayer structures [3, 4] and prisms [5, 7], where negative refraction at the output interface of the prism has been reported. Although the relation between negative refractive index in fishnet structures and extraordinary optical transmission through metallic plates perforated by periodic hole arrays [9] was clear from the beginning [2], the first attempts to explain the behavior of fishnet structures followed the standard interpretation of negative refraction in wire and split ring metamaterials [10]. Thus, the straight conducting strips of the fishnets were supposed to act as a "wire medium" providing a negative ϵ , whereas the coupled metallic strips along the orthogonal direction were supposed to form an LC resonator providing a negative μ [1, 2, 6–8]. This interpretation, however, could not explain why the transverse periodicity of all fishnet metamaterials was close to a wavelength in all reported experiments and electromagnetic simulations. For this reason, other interpretations linking the behavior of stacked fishnet metamaterials to the presence of extraordinary optical transmission through a single layer fishnet have been proposed [3, 5, 11].

The main aim of this letter is to develop an analytical theory of wave propagation through stacked fishnet structures from zero frequency to the first Wood's anomaly. The analysis will start with a canonical structure (a periodic arrangement of single fishnets of square periodicity and negligible thickness) showing the most important properties of these stacked fishnets. This analysis generalizes our previous analysis of extraordinary transmission through metallic plates perforated by periodic hole arrays [12, 13], and shows that extraordinary transmission in single-layer fishnets and extraordinary propagation in stacked fishnets can both be explained within the same theoretical framework. From this analysis, closed-form expressions for the dispersion relation of an infinite periodic array of single-layer fishnets will be derived. After careful testing of these expressions by appropriate numerical simulations, they will be discussed and the main physical mechanisms behind wave propagation through stacked fishnet metamaterials will be identified. Finally, the analysis will be generalized to structures of higher complexity.

2. Analysis

For the sake of simplicity we begin our analysis with the structure shown in Fig.1 assuming negligible thickness and square holes perforated in a periodic array of perfectly conducting metallic screens. Propagation along the normal direction (i.e. along z axis) will be considered, with a time dependence $\propto \exp(-i\omega t)$. The unit cell of this structure is also shown in Fig.1(c) and (d).

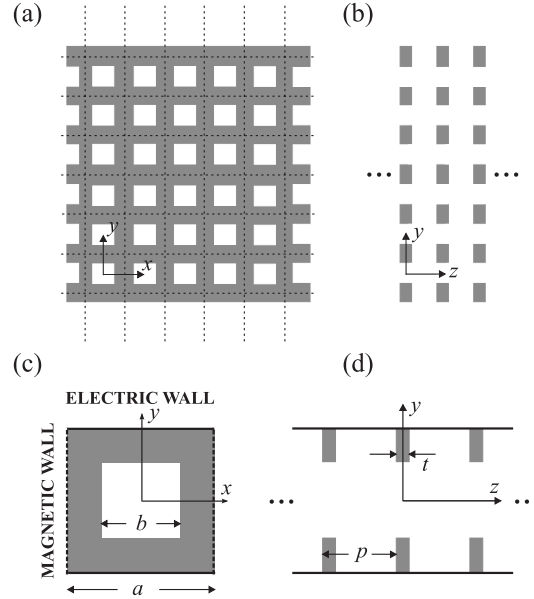


Fig. 1. Periodic array of perfect conductor screens perforated with square holes: (a) front view and (b) lateral view. (c) Front and (d) lateral views of the structure unit cell or equivalent waveguide.

For propagation along the z axis the structure and the field are both invariant by reflections at the $x = \pm a/2$ and $y = \pm a/2$ planes. Owing to the specific properties of electric and magnetic fields under mirror symmetry [14, pp. 267-273], these planes must be virtual perfect electric or perfect magnetic conducting (PEC or PMC) walls. Choosing x -planes as PMCs and y -planes as PECs we obtain the unit cell depicted in Fig.1(c) and (d), which implies an y -polarized mode. It is also possible to make the opposite choice for the x - and y - planes, which leads to the orthogonal propagating mode (which, for the considered square periodicity, has the same dispersion equation). Choosing x - and y -planes both as PECs (or PMCs) leads - below Wood's anomaly - to non propagative modes, which will not be considered here. Thus, for the considered propagation, the analyzed structure is equivalent to the TEM square waveguide periodically loaded by square irises shown in Fig.1(c) and (d).

Following our previous analysis [13], the electric field, E_y^0 , produced by the currents flowing on the metallic screen at $z = 0$ (see Fig.1) is expanded as the following series of the TEM, $TE_{2n,2m}$, and $TM_{2n,2m}$ modes of the infinite TEM waveguide with appropriate coefficients:

$$E_y^0(x,y) = A_0 + \sum_{n=1}^N A_{n0}^{TE} f_{n0}(x,y) + \sum_{m=1}^M A_{0m}^{TM} f_{0m}(x,y) + \sum_{n,m=1}^{N,M} (A_{nm}^{TE} + A_{nm}^{TM}) f_{nm}(x,y) \quad (1)$$

where

$$f_{nm}(x,y) = \cos(2n\pi x/a) \cos(2m\pi y/a) \quad (2)$$

gives the the dependence on x, y of the different $TE_{2n,2m}$ and $TM_{2n,2m}$ modes of the waveguide. In (1) only even modes have been considered due to the symmetry of the structure, which includes two additional symmetry planes at $x = 0$ and at $y = 0$, respectively. From (1), using standard waveguide theory, the electric field component E_x^0 produced by these currents is written as

$$E_x^0(x, y) = \sum_{n,m=1}^{\infty} \left(\frac{m}{n} A_{nm}^{TE} - \frac{n}{m} A_{nm}^{TM} \right) g_{nm}(x, y) \quad (3)$$

where $g_{nm}(x, y) = \sin(2n\pi x/a) \sin(2m\pi y/a)$.

Let us now assume that a Bloch wave of phase dependence $e^{i\beta z}$ is propagating along the structure. The total field at $z = 0$ is given by the addition of (1) and the *incident* field, E_y^{inc} , created by the currents on all the remaining screens at $z = qp$, where p is the periodicity along the z -axis and $q = \pm 1, \pm 2, \dots$. Near Wood's anomaly, where the first higher order modes TE_{20} and TM_{02} in the expansion (1) are at cutoff, the attenuation constant of such modes

$$\alpha = k_0 \sqrt{\left(\frac{\lambda}{a}\right)^2 - 1} ; \quad k_0 = \omega \sqrt{\epsilon_0 \mu_0} \quad (4)$$

is very small and these modes contribute to the incident field at $z = 0$ regardless of the periodicity of the structure. Thus, for not very small periodicities, where additional higher order modes may be present, the incident field at $z = 0$ can be expressed as

$$E_y^{\text{inc}} = E_y^{\text{TEM}} + E_y^{\text{TE}} + E_y^{\text{TM}} \quad (5)$$

where

$$E_y^{\text{TEM}} = \sum_{q \neq 0} A_0 e^{i\beta qp} e^{ik_0|q|p} = A_0 \frac{\cos(\beta p) - e^{ik_0 p}}{\cos(k_0 p) - \cos(\beta p)} \quad (6)$$

$$E_y^{\text{TE}} = \sum_{q \neq 0} A_{10}^{\text{TE}} f_{10} e^{i\beta qp} e^{-\alpha|q|p} = A_{10}^{\text{TE}} f_{10} \frac{\cos(\beta p) - e^{-\alpha p}}{\cosh(\alpha p) - \cos(\beta p)} \quad (7)$$

$$E_y^{\text{TM}} = \sum_{q \neq 0} A_{01}^{\text{TM}} f_{01} e^{i\beta q} e^{-\alpha|q|p} = A_{01}^{\text{TM}} f_{01} \frac{\cos(\beta p) - e^{-\alpha p}}{\cosh(\alpha p) - \cos(\beta p)}. \quad (8)$$

The presence of the terms E_y^{TE} and E_y^{TM} in the incident field at $z = 0$ makes our analysis different from the standard analysis of periodic structures [16, Sec. 9], which usually only considers the coupling through the fundamental TEM mode of the waveguide. As it will be shown in the following, it is the coupling through the TM_{02} mode what creates a transmission band starting at Wood's anomaly which, depending on the structural parameters, can provide a backward wave propagating along the stacked fishnet.

After this point the analysis follows the same procedure as in [13]. First, the coefficients of (1) are obtained in the frame of the small hole approximation. In this approximation the x component of the electric field (3) is $E_x(x, y)^0 \approx 0$, which follows from the boundary conditions at the metallic screen, and from the specific behavior of $g_{nm}(x, y)$ for $x, y \approx 0$. This approximation gives the relation

$$\frac{m}{n} A_{nm}^{\text{TE}} - \frac{n}{m} A_{nm}^{\text{TM}} \approx 0 ; \quad n, m \neq 0. \quad (9)$$

In order to complete the determination of the coefficients, we make use of the approximation [15]:

$$\iint_w E_y f_{nm} dx dy = \iint_h E_y f_{nm} dx dy \approx \iint_h E_y dx dy = \iint_w E_y dx dy \quad (10)$$

where $E_y = E_y^0 + E_y^{\text{TEM}} + E_y^{\text{TE}} + E_y^{\text{TM}}$ is the total field at $z = 0$, and subindex w and h stand for the waveguide and hole sections respectively. This condition provides the equation

$$\iint_w E_y f_{nm} dx dy = a^2 A_0 \left(1 + \frac{\cos(\beta p) - e^{ik_0 p}}{\cos(k_0 p) - \cos(\beta p)} \right) \quad (11)$$

which, after expanding E_y in a series similar to (1) and using the orthogonality properties of f_{nm} , suffices for the determination of all the coefficients as a function of the first coefficient A_0 . Once all coefficients in (1) have been determined, the tangential magnetic field created by the currents at $z = 0$, H_x^0 , is obtained from (1) using waveguide theory [16, Sec. 5]. Finally, the phase constant β of the Bloch wave is obtained by imposing the condition $H_x^0 = 0$ at the aperture [14, p. 486]. After some cumbersome but straightforward calculations, the dispersion equation for the Bloch wave can be written in the following way:

$$\cos(\beta p) = 1 + \frac{Y_p}{Y_s} \quad (12)$$

where

$$Y_p = -2iY_0 \frac{\sin^2(k_0 p/2)}{\sin(k_0 p)} + 4(Y_{20}^{\text{TE}} + Y_{02}^{\text{TM}}) \frac{\sinh^2(\alpha p/2)}{\sinh(\alpha p)} \text{sinc}\left(\frac{\pi b}{a}\right) + Y \quad (13)$$

$$Y_s = iY_0 \csc(k_0 p) + 2(Y_{20}^{\text{TE}} + Y_{02}^{\text{TM}}) \text{csch}(\alpha p) \text{sinc}\left(\frac{\pi b}{a}\right) \quad (14)$$

with $\text{sinc}(x) = \sin(x)/x$, and

$$Y = 2 \sum_{n=2}^N Y_{2n,0}^{\text{TE}} \text{sinc}\left(\frac{n\pi b}{a}\right) + 2 \sum_{m=2}^M Y_{0,2m}^{\text{TM}} \text{sinc}\left(\frac{m\pi b}{a}\right) + 4 \sum_{n,m=1}^{N,M} \left(Y_{2n,2m}^{\text{TE}} \frac{n^2}{n^2 + m^2} + Y_{2n,2m}^{\text{TM}} \frac{m^2}{n^2 + m^2} \right) \text{sinc}\left(\frac{n\pi b}{a}\right) \text{sinc}\left(\frac{m\pi b}{a}\right) \quad (15)$$

where $Y_0 = \sqrt{\epsilon_0/\mu_0}$ is the wave admittance of free space, and $Y_{2n,2m}^{\text{TE}}$ and $Y_{2n,2m}^{\text{TM}}$ are the admittances of the TE and TM waveguide modes given by

$$Y_{2n,2m}^{\text{TE}} = iY_0 \sqrt{\left(\frac{n\lambda}{a}\right)^2 + \left(\frac{m\lambda}{a}\right)^2 - 1} \quad (16)$$

$$Y_{2n,2m}^{\text{TM}} = -iY_0 / \sqrt{\left(\frac{n\lambda}{a}\right)^2 + \left(\frac{m\lambda}{a}\right)^2 - 1} \quad (17)$$

and the upper limits of the summations in (15) are taken as $N, M = \text{round}(a/b)$ [13]. It should be emphasized that, for practical values of a and b , the value of N, M is usually very low (no more than five or six), which means that very few terms should be summed up in the series in (15).

3. Discussion and numerical results

The dispersion equation (12) formally corresponds to the periodic equivalent circuit whose unit cell is shown in Fig.2(a) [16, Sec. 9], which takes the well known form

$$\beta p = \sqrt{-\frac{2Y_p}{Y_s}} \quad (18)$$

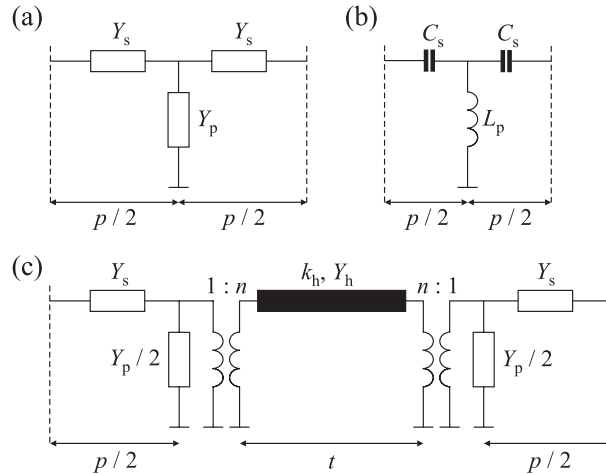


Fig. 2. Unit cells of (a) the periodic transmission line corresponding to the dispersion equation (12) for a stacked fishnet with $t \rightarrow 0$, (b) the backward-wave transmission line reported and analyzed in [17, pp. 263-264] and [18], (c) the equivalent circuit proposed in Sec. 4 for thick stacked fishnet.

in the limit of electrically small periodicities ($\beta p \ll 1$). This last equation corresponds to an infinite transmission line of periodicity p , parallel admittance Y_p , and series admittance $2Y_s$.

The interpretation of the different admittances in (13)–(15) is straightforward. The parallel admittance (13) has three terms. The third term Y is the contribution of all the waveguide modes localized at the discontinuities, *i.e.*, of all the $TE_{2n,2m}$, and $TM_{2n,2m}$ modes with $n + m > 1$. The first and the second terms in (13) correspond to the contributions of the non-localized modes, *i.e.*, the TEM, TE_{20} , and TM_{02} modes. As expected, only these non localized modes contribute to the series admittance (14). The main difference between these equations and the standard equations for periodically loaded transmission lines and waveguides [16, Sec. 9] is the presence of the non-localized TE_{20} and TM_{02} modes in the series admittance Y_s . As it was already mentioned, this presence is imposed by the small values of the attenuation constant (4) near Wood's anomaly, and it provides the most relevant physical effects in stacked-fishnet structures. In particular, just at Wood's anomaly, the attenuation constant (4) vanishes and the corresponding TM_{02} mode admittance (17) becomes infinite. Also the series admittance Y_s (14) becomes infinite and the phase constant β vanishes. Hence, there is always a transmission band starting at Wood's anomaly with zero phase and group velocity. Just below Wood's anomaly, the series admittance is dominated by the TM_{02} admittance, which is capacitive ($\Im(Y_{02}^{TM}) < 0$). Thus, if the parallel admittance is inductive ($\Im(Y_p) > 0$), according to (18) there must be a backward-wave transmission band [17, pp. 263-264] just below Wood's anomaly. Now we will examine under which conditions the parallel admittance is inductive. For small holes, the contribution of the localized modes (15) is always inductive [12, 16]. For small values of the longitudinal periodicity p , the contribution of the two first terms in (13) is negligibly small (of the order of $Y_0 k_0 p$). Therefore, for small holes and periodicities, a backward-wave transmission band is always expected just below Wood's anomaly.

After the discussion of some of the qualitative predictions of our analytical model, some numerical results will be presented next. Thus, Fig. 3 and Fig. 4 show some dispersion diagrams for the stacked-fishnet structure shown in Fig. 1 for different structural parameters. For comparison purposes, results obtained using the commercial electromagnetic solver CST Microwave Studio are also shown. These plots qualitatively confirm the abovementioned backward-wave behav-

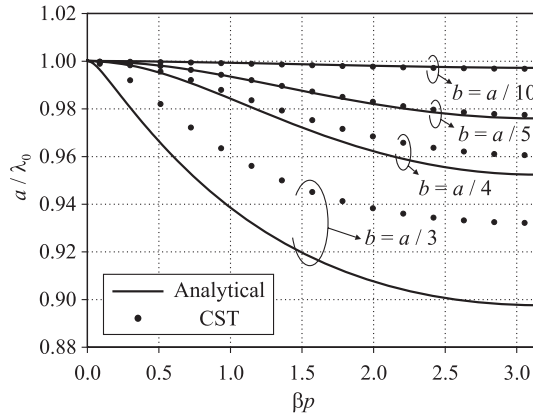


Fig. 3. Dispersion diagrams for a periodic array of stacked fishnets as that shown in Fig.1 with negligible thickness $t \rightarrow 0$, periodicity $p = a/3$, and different values of the hole size b . Solid lines are calculated using formulas (12)–(15). Circles correspond to numerical simulations by CST Microwave Studio.

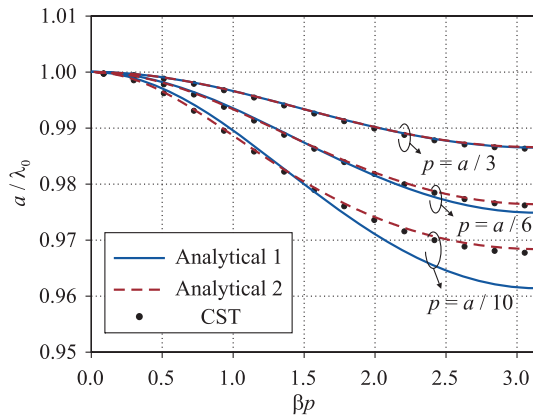


Fig. 4. Dispersion diagrams for a periodic array of stacked fishnets as that shown in Fig.1 with negligible thickness $t \rightarrow 0$, hole size $b = a/6$, and different values of the periodicity p . Blue solid lines (Analytical 1) are calculated using formulas (12)–(15). Red dashed lines (Analytical 2) are obtained using (20)–(21) for the parallel and series admittances. Circles correspond to numerical simulations by CST Microwave Studio.

ior, and also show a good quantitative agreement in most cases. The disagreement between the analytical and intensive numerical computations for the biggest hole sizes shown in Fig. 3 can be attributed to the approximations made in our model. In fact, approximation (10) is expected to work properly only for small holes [15]. In Fig. 4 there is also some disagreement between the numerical values obtained from formulas (12)–(15) [the curve denoted as “Analytical 1”] and the CST numerical computations, specifically for small periodicities. This disagreement is explained by the extra coupling between consecutive screens by higher order modes. When this extra coupling is taken into account (see Section 4) these discrepancies disappear [as shown by the satisfactory agreement between the so-called “Analytical 2” curve and the CST results]. Figs. 3 and 4 also show that the bandwidth of the backward transmission band increases as the hole size increases but it decreases as the periodicity grows.

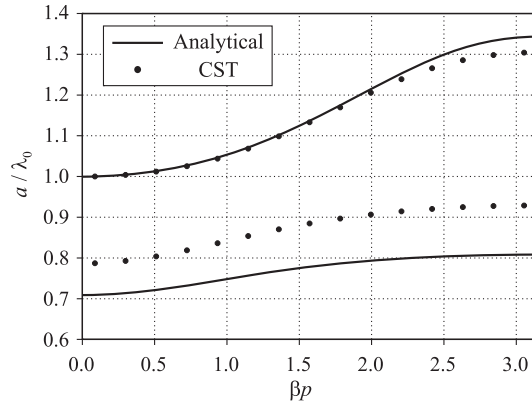


Fig. 5. Dispersion diagrams for a periodic array of stacked fishnets as that shown in Fig.1 with negligible thickness $t \rightarrow 0$, hole size $b = a/2$, and periodicity $p = a/3$. Solid lines were calculated using formulas (12)–(15). Circles correspond to numerical simulations by CST Microwave Studio.

As is well known, the holes become resonant when their size approaches to a half-wavelength. Below Wood’s anomaly, this situation only occurs if $b \gtrsim a/2$. In that case, there appears an additional transmission band associated with the resonance of the holes. In our model, the appearance of this additional transmission band can be linked to a zero value of the parallel admittance Y_p in (12). Since the presence of this zero causes a change of sign in the parallel admittance, the transmission band starting at Wood’s anomaly will be forward. However the nature of the transmission band related to the resonance of the hole cannot be predicted in advance as it will depend on the sign of the series admittance. This last behavior is shown in Fig. 5, where two forward transmission bands (one of them starting at Wood’s anomaly) can be seen. The agreement between our analytical results and the numerical simulations is still quite good in Fig. 5, in spite of the fact that now the approximation (10) can be hardly justified. This agreement is surprisingly good for the upper band as $\beta p \lesssim 2$. When the periodicity p becomes a multiple of a half-wavelength, our analytical model still predicts the expected additional narrow transmission bands linked to Fabry-Perot resonances (their nature can be forward/backward depending on the longitudinal periodicity). However, the study of this kind of resonances is beyond the scope of the present work.

In summary, there can be three independent mechanisms for electromagnetic wave propagation through stacked-fishnet structures operating below or near Wood’s anomaly. One of them is associated with the pole that appears in the first evanescent TM mode admittance just at Wood’s anomaly, and it is always present regardless of the hole size and periodicity p . The second one is related to the resonances of the holes, and appears as the hole size approaches to a half of the transverse periodicity a . Finally, when the longitudinal periodicity p becomes a multiple of a half-wavelength, narrow transmission bands linked to Fabry-Perot resonances appear. Note that in all the above mechanisms one or more of the periodicities are not electrically small. Therefore, stacked-fishnet structures cannot be homogenized, at least when “homogenization” is taken in its usual meaning. However, the two first abovementioned mechanisms of wave propagation are compatible with an electrically small longitudinal periodicity p . In this case, the dispersion equation can be approximated by (18). Under this approximation, and assuming that the resulting transmission band is backward, the stacked-fishnet structure behaves like the backward-wave transmission line whose unit cell is sketched in Fig. 2(b). These transmission lines are well known by electrical engineers, and have been analyzed in many textbooks [17, pp.

263-264]. More recently, they have been proposed as an alternative way to obtain left-handed metamaterials (see [18] and references therein) operating at microwave frequencies. Thus, in this specific case and in this specific sense, the stacked-fishnet structure can be considered as a 1D left-handed metamaterial with effective permittivity, ϵ , and permeability, μ , given by [18]

$$\epsilon = -\frac{1}{\omega^2 L_p p}, \quad \mu = -\frac{2}{\omega^2 C_s p} \quad (19)$$

where C_s and L_s come from $Y_s = -i\omega C_s$ and $1/Y_p = -i\omega L$.

An additional conclusion of our analysis is that backward-wave propagation in stacked fishnets can be dealt within the same theoretical framework as extraordinary transmission through single-layer fishnets (see [12] and [13]). It also shows that the physical mechanism behind this behavior is not linked to the presence of any kind of *LC* resonant circuits, as it was proposed in many previous works [1, 2, 6–8]. On the contrary, backward-wave propagation in stacked fishnets closely resembles backward-wave propagation in transmission line metamaterials [18], as it was previously suggested in [3].

4. Generalization of the analysis

The analysis of the canonical structure studied in Section 2 has shown the most salient features of stacked fishnets, and has provided qualitative results that can easily be generalized to more specific structures. In this section, this analysis will be extended to more general configurations. These generalizations include thick screens, arbitrary periodicities in the transverse plane, rectangular holes, and very small longitudinal periodicities. In all these generalization, the metallic screens will still be considered as perfect conductors. Since the same phenomena observed in stacked fishnets at infrared and optical frequencies were also observed at RF and microwave frequencies, where metallic screens are almost perfect conductors, we feel that the main conclusions extracted from our analysis can also be generalized to the optical range, at least qualitatively.

For arbitrary periodicities along the x and y axes, a_x and a_y , and for rectangular holes of dimensions b_x and b_y along these axes, the generalization of (12)–(15) is straightforward. Moreover, if the periodicity along the longitudinal direction p is small, coupling between the metallic screens by higher order evanescent modes may appear. Specifically, this coupling will appear when the product $\alpha_{nm}p$ is small, where $\alpha_{nm} = k_0 \sqrt{(n\lambda/a_x)^2 + (m\lambda/a_y)^2 - 1}$ is the attenuation constant of the $TE_{2n,2m}$ or $TM_{2n,2m}$ modes. For the above cases, the analysis leads to the following general expressions for Y_p and Y_s in (12):

$$\begin{aligned} Y_p = & -2i \frac{a_x}{a_y} Y_0 \frac{\sin^2(k_0 p/2)}{\sin(k_0 p)} \\ & + 4 \frac{a_x}{a_y} \sum_{n=1}^N Y_{2n,0}^{TE} \frac{\sinh^2(\alpha_{n0} p/2)}{\sinh(\alpha_{n0} p)} \operatorname{sinc}\left(\frac{n\pi b_x}{a_x}\right) + 4 \frac{a_x}{a_y} \sum_{m=1}^M Y_{0,2m}^{TM} \frac{\sinh^2(\alpha_{0m} p/2)}{\sinh(\alpha_{0m} p)} \operatorname{sinc}\left(\frac{m\pi b_y}{a_y}\right) \\ & + 8 \frac{a_x}{a_y} \sum_{n,m=1}^{N,M} \left(Y_{2n,2m}^{TE} \frac{n^2}{n^2 + m^2} + Y_{2n,2m}^{TM} \frac{m^2}{n^2 + m^2} \right) \frac{\sinh^2(\alpha_{nm} p/2)}{\sinh(\alpha_{nm} p)} \operatorname{sinc}\left(\frac{n\pi b_x}{a_x}\right) \operatorname{sinc}\left(\frac{m\pi b_y}{a_y}\right) \end{aligned} \quad (20)$$

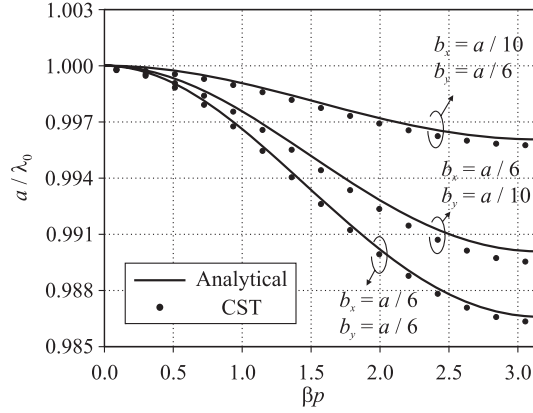


Fig. 6. Dispersion diagrams for a periodic array of stacked fishnets as that shown in Fig.1 with negligible thickness $t \rightarrow 0$, periodicity $p = a/3$, and three different rectangular hole sizes. Solid lines were calculated using formulas (12) and (20),(21). Circles correspond to numerical simulations obtained by CST Microwave Studio.

$$\begin{aligned}
 Y_s = & i \frac{a_x}{a_y} Y_0 \csc(k_0 p) \\
 & + 2 \frac{a_x}{a_y} \sum_{n=1}^N Y_{2n,0}^{\text{TE}} \text{csch}(\alpha_{n0} p) \text{sinc}\left(\frac{n\pi b_x}{a_x}\right) + 2 \frac{a_x}{a_y} \sum_{m=1}^M Y_{0,2m}^{\text{TM}} \text{csch}(\alpha_{0m} p) \text{sinc}\left(\frac{m\pi b_y}{a_y}\right) \\
 & + 4 \frac{a_x}{a_y} \sum_{n,m=1}^{N,M} \left(Y_{2n,2m}^{\text{TE}} \frac{n^2}{n^2 + m^2} + Y_{2n,2m}^{\text{TM}} \frac{m^2}{n^2 + m^2} \right) \text{csch}(\alpha_{nm} p) \text{sinc}\left(\frac{n\pi b_x}{a_x}\right) \text{sinc}\left(\frac{m\pi b_y}{a_y}\right).
 \end{aligned} \tag{21}$$

The factor a_x/a_y in (20) and (21) does not play any role in the dispersion equation. However, the introduction of this factor is convenient in order to make the admittances consistent with its circuit definition, namely, the ratio between the average current and the average voltage through the waveguide. Note that (20) and (21) reduces to (13) and (14) as $\alpha_{nm}p$ increases up to a value that there is no coupling through the corresponding mode.

When the dispersion diagrams of Fig. 4 are computed using (20) and (21) instead of (13) and (14), the plotted results are the red dashed curves also shown in Fig. 4. As it can be seen, for small periodicities p , the introduction of this additional coupling substantially improves the quantitative agreement with numerical simulations. New dispersion diagrams for a stacked fishnet structure with rectangular holes have also been computed. The results are shown in Fig. 6. This Figure shows that there is again a satisfactory qualitative and quantitative agreement with numerical simulations.

Finally, the analysis can also be generalized to the case of thick screens using the equivalent circuit proposed in [12] and [13] for the analysis of extraordinary transmission through thick screens. This equivalent circuit is shown in Fig.2(c), where the transformer turns ratio is $n = a_x/b_x$ and the transmission line admittance, defined as the ratio between the average current and the average voltage through the rectangular waveguide of length t , is $Y_h = Y_{\text{TE}_{10}}(b_y/b_x)$, where $Y_{\text{TE}_{10}}$ is the wave admittance of the fundamental TE_{10} mode excited in the waveguide formed by the hole in the screen. After solving the circuit of Fig.2(c), it turns out that this circuit can still be represented by the elemental circuit of Fig.2(a), provided the original series and parallel

admittances Y_s and Y_p are substituted by the following new series and parallel admittances:

$$Y'_s = \left\{ \frac{1}{Y_s} + \frac{-iY_p \sin(k_h t) + 2Y_h (\cos(k_h t) - 1)}{(Y_p/2 + Y_h) 2e^{-ik_h t} - (Y_p/2 - Y_h) 2e^{ik_h t}} \right\}^{-1} \quad (22)$$

$$Y'_p = \frac{(Y_p/2 + Y_h) 2e^{-ik_h t} - (Y_p/2 - Y_h) 2e^{ik_h t}}{2Y_h} \quad (23)$$

where k_h is the phase constant of the fundamental TE_{10} mode excited in the hole-waveguide through the screen. In Fig. 7 it is shown the dispersion diagrams for two similar fishnet structures with negligible thickness, and with finite thickness ($t \neq 0$). It is apparent that the finite thickness of the screen strongly affects the dispersion diagram, a fact that can somewhat be expected by the strong attenuation of the electromagnetic fields through the hole. The reduction in the bandwidth of the passband as t increases can be understood by linking the stacked fishnet problem to the single-layer fishnet problem. In this way, it should be noted that, not very close to the Wood's anomaly (and also in the long-wavelength limit), the single-layer fishnet problem with only TEM incident fields can be considered as the unit cell of the longitudinally periodic problem appearing in the stacked fishnet problem. Now it should be reminded that in the single-layer fishnet problem it was already reported that the screen thickness gives rise to two peaks of extraordinary transmission instead of the single one observed for infinitesimally thin screens. According to the equivalent circuits proposed in [12, 13], the evolution of these two peaks with respect to the increasing screen thickness is the following. One peak moves from the position it has for $t = 0$ in the direction of the Wood's anomaly. The other peak moves from the Wood's anomaly in the reverse direction. (Certainly the case $t = 0$ can be considered as the limiting case as $t \rightarrow 0$ in such a way that one of the two peaks coincides with the Wood's anomaly). It means that the two extraordinary-transmission peaks tend to approach each other until, eventually, they collapse in one single peak of partial transmission [12, Fig.6]. In other words, the "distance" between the two peaks decreases as the screen thickness increases. Considering now the connection between the single-layer and the stacked fishnet problems, it can easily be deduced that the two peaks of extraordinary transmission of the single-layer fishnet turn out to be the lower and upper limit of the transmission band observed in the stacked fishnet problem. Thus the corresponding reduction of the "distance" between the two peaks in the single-layer fishnet problem as the screen thickness increases is directly related to the decrease of the passband bandwidth observed in the stacked fishnet problem.

As in previous cases, a good qualitative agreement between our analytical results and the CST numerical results can be observed in Fig. 7. Definitely, a better quantitative agreement could be obtained by adjusting some parameters, such as the turns ratio of the transformers (which was based on a quite rough approximation [13]).

5. Conclusions

Stacked fishnets have been previously proposed as an alternative way to negative refractive index metamaterials. Along this paper we have developed an analytical theory of electromagnetic wave propagation through stacked fishnet structures made of perfect conducting screens. Since the same phenomena observed at optical frequencies were also observed in the microwave range, where metals are almost perfect conductors, we feel that the main results of our analysis can be extended to stacked fishnets operating in the optical range, at least qualitatively.

Our analysis generalizes our previous work on extraordinary optical transmission through single layer fishnets, also making apparent the close relation between both phenomena. It has been shown that there can be three mechanisms of wave propagation through stacked fishnet metamaterials. First of all there is the extra coupling between screens through the first excited

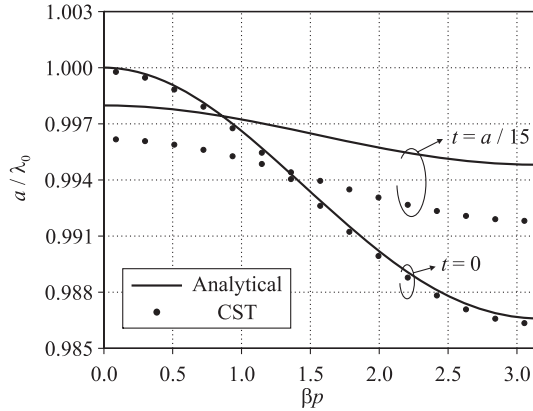


Fig. 7. Dispersion diagrams for a periodic array of stacked fishnets as that shown in Fig.1 with periodicity $p = a/3$ and hole size $b = a/6$. Two different screen thicknesses have been considered. Solid lines correspond to our analytical formulas. Circles correspond to numerical simulations obtained by CST Microwave Studio.

higher order TM mode of the structure (the TM_{02} mode) near Wood's anomaly. Due to this additional coupling, a frequency transmission band starting at Wood's anomaly with zero phase and group velocity is always present in zero-thickness stacked fishnets. It has been shown that this transmission band is always backward for small or moderate hole sizes and longitudinal periodicities. Besides this mechanism, which is closely linked to extraordinary transmission through single layer fishnets with subwavelength holes, there are other two possible physical mechanisms. One of them is associated with the resonances of the holes. The other is related to the Fabry-Perot resonances of the whole structure along the longitudinal direction. In all the above mechanisms it is implicitly assumed that at least one periodicity of the whole 3D structure is electrically large. Therefore, a stacked fishnet structure can never be considered as a 3D effective medium. However, when the longitudinal periodicity of the structure can be made electrically small, the equations governing the wave propagation through the stacked fishnets are found to be formally equivalent to the equations governing the wave propagation through the well-known backward-wave transmission lines [17, pp. 263-264]. These latter transmission lines have been recently proposed for obtaining 1D left-handed metamaterials at RF and microwave frequencies [18]. Thus, stacked fishnets appear as a specific realization of this concept, allowing operation not only at RF and microwave frequencies but also in the optical range.

Acknowledgments

This work has been supported by the Spanish Ministerio de Educación y Ciencia and European Union FEDER funds (projects TEC2007-65376, TEC2007-68013-C02-01, and CSD2008-00066), and by Junta de Andalucía (project TIC-253). L. Jelinek also thanks for the support of the Czech Grant Agency (project no. 102/08/0314).